Pharm Res (2013) 30:3238–3253
DOI 10.1007/s11095-013-1206-1

RESEARCH PAPER

Glyceride Lipid Formulations: Molecular Dynamics Modeling of Phase Behavior During Dispersion and Molecular Interactions Between Drugs and Excipients

Dallas B. Warren • Dylan King • Hassan Benameur • Colin W. Pouton • David K. Chalmers

Received: 6 January 2013 / Accepted: 12 September 2013 / Published online: 3 October 2013

ABSTRACT

Purpose Little is known about the microstructure of lipid-based formulations, or how their structure changes as they disperse in the lumen of the gastrointestinal tract. We used molecular dynamics (MD) simulation to study such formulations at the molecular level as they interact with water during dispersion.

Methods We studied a simple lipid formulation, by itself and in the presence of drugs. The formulation contained mono- and dilauroyl glycerides at 0–75% $^{w}/_{w}$ water. Acyclovir, danazol, hydrocortisone, ketoprofen or progesterone, were included to investigate their dynamic behavior and localization during dispersion.

Results Micro-structuring of the formulation was evident at all water concentrations. As the water content increased, the microstructure evolved from a continuous phase containing isolated water molecules, to a reverse micellar solution and finally to a system containing lamellar lipids with large pools of free water. Drugs partitioned into the aqueous and lipid domains principally under the influence of hydrogen bonding and hydrophobic interactions. Drugs located preferentially to the interfaces between water and lipid where they are able to make both hydrophobic and hydrophilic interactions.

Conclusion Molecular dynamics simulations offer an unprecedented view of the structure of lipid-based formulations and has considerable potential as an *in silico* tool for formulators.

Electronic supplementary material The online version of this article (doi:10.1007/s11095-013-1206-1) contains supplementary material, which is available to authorized users.

D. B. Warren • C. W. Pouton (✉)
Drug Discovery Biology, Monash Institute of Pharmaceutical Sciences
Monash University, Parkville Campus, Melbourne, Victoria, Australia
e-mail: colin.pouton@monash.edu

D. King • D. K. Chalmers (✉)
Medicinal Chemistry, Monash Institute of Pharmaceutical Sciences
Monash University, Parkville Campus, Melbourne, Victoria, Australia
e-mail: david.chalmers@monash.edu

H. Benameur
Pharmaceutical Sciences, Capsugel R&D, Strasbourg, France

KEY WORDS drug microenvironment · lipid-based formulations · microemulsions · molecular dynamics · phase behavior

INTRODUCTION

Molecular dynamics (MD) simulations are an important tool for investigating the phase behavior of liquid and liquid crystal systems. Among many areas of application, MD has great potential as a tool for predicting the micro-structure of lipid-based drug formulations (1–3). In particular MD has the potential to provide details of molecular interactions within formulations that cannot be revealed by spectroscopic techniques or X-ray diffraction. The internal structure of mixtures of excipients that form a single phase often cannot be studied by physical analysis due to the large number of different molecular species present. In contrast, MD can reveal the internal structure of oil-continuous inverted micellar or microemulsion systems, which are often present in lipid-based formulations (1). MD can provide information about the distribution of drugs within the formulation and reveal changes in microstructure caused by the drug. MD simulations can also be used to model the events that occur on dispersion and digestion of the formulation in the gastrointestinal tract; to model the fate of poorly water soluble drugs that are prone to precipitation.

Although MD has great potential in this field, until recently the considerable computing power required to run MD calculations of model lipid systems has limited progress. At this stage there are a limited number of publications exploring the use of MD in pharmaceutical formulations (1,4–6). It would be very useful if the fate of a poorly water soluble drug could be predicted during its transit within the gastrointestinal tract prior to, and including, absorption. The effects of food on absorption will be too complex to simulate for some time, but it may be possible to model the effects of bile and lipid

digestion on the formulations in the near future. However, at present little is known about modelling the dispersion phase and this requires better understanding before attempting to model the intestinal digestion of formulations. This paper focuses on the internal structure of formulations, the distribution of drugs within them, and how the system changes as formulations make contact with water.

The objective of a lipid formulation is to present a poorly water-soluble drug to the gastrointestinal lumen in colloidal solution, avoiding the slow process of dissolution from a crystalline form which often results in poor bioavailability. Upon dispersion of the lipid formulation in the gastrointestinal lumen and subsequent digestion, the solvating properties of the formulation may change, leading to a chance of precipitation of the drug, at which point the advantage of the lipid formulation is lost. Care is required with design of the formulation, because if the focus is to maximise the mass of drug in the formulation, without consideration of the performance upon dispersion and digestion, then the performance of the product *in vivo* may be poor.

A variety of excipients can be included within lipid formulations and it is the relative amounts of these compounds that is currently used to categorize these formulations through the Lipid Formulation Classification System, which has been developed to assist in the prediction of *in vivo* performance (7,8). Type I formulations consist of oils, including various ratios of mono-, di- and tri-glycerides. Type II formulations are water insoluble self-emulsifying drug delivery systems (SEDDS) consisting of oils with water insoluble surfactants (hydrophobic lipophilic balance, HLB, less than 12). Type III formulations are self-microemulsifying drug delivery systems (SMEDDS) containing water soluble surfactants (HLB greater than 12) with a hydrophilic cosolvent and are divided into two subclasses where Type IIIA has a larger proportion of oils and Type IIIB a greater proportion of water soluble surfactant. Finally, Type IV lipid formulations consist of hydrophilic surfactants and hydrophilic cosolvents and no oils.

In this work we have MD simulations to study the molecular behavior of a model Type I lipid formulation consisting of 1:1 molar ratio mixture of mono-lauroyl glyceride (MGL) and di-lauroyl glyceride (DGL). The structures of these lipids are shown in Fig. 1. Both glycerides are esters of the saturated C12 fatty acid, lauric or dodecanoic acid. This lipid mixture is representative of a Type I lipid formulation (8), which is typically composed of mixed glycerides (7). To model the process of initial dispersion of the formulation within the aqueous phase of the gastrointestinal tract, we have performed multiple simulations of the formulation/water mixtures ranging from 0 to 75% $^{w}/_{w}$ water. This has allowed us to study the process of water uptake into Type I formulations and to explore the concentrations at which the system forms reverse micelles, micro-emulsions and ultimately phase separates to form discrete small emulsion droplets. The dispersion of a lipid formulation within the gastro intestinal tract would typically result in ~99.6% $^{w}/_{w}$ water; based on a 1 g lipid formulation capsule dispersing into 250 cm^3 of gastro intestinal contents. At such high water concentrations, nearly all the computing time is spent calculating water-water interactions and we have chosen a maximum water concentration of 75%. The phase behaviour of the mono and di-glycerides with water systems do not exhibit a change in phase behaviour beyond 20 to 70% $^{w}/_{w}$ water (9).

The Type I formulation modeled here has previously been investigated using a limited range of concentrations but the current work has been performed using longer simulations (100 *versus* 40 ns), more concentrations (10 *versus* 6), and better simulation methods; improved treatment of electrostatic interactions (PME *versus* cut-offs), and better temperature coupling (velocity rescaling with separate temperature coupling groups for individual chemical components *versus* the Berensden method applied to the entire system) and pressure coupling techniques (Parrinello-Rahman *versus* Berensden method). An important reason for choosing Type I formulations for this study was that the modelling parameters for simple glycerides have been optimised adequately in previous studies. Parameters for the MD modelling of non-ionic surfactants based on polyoxyethylene chains, which are major components of Type II, III and IV lipid systems, need to be optimized and validated before MD can be used with confidence for modelling such systems.

Using the model Type I lipid formulation we have also studied the partitioning behavior of five different drugs during dispersion. The drugs were selected to cover a range of different drug classes that might be considered for inclusion within lipid formulations. The selected compounds in order of increasing logP are; acyclovir (hydrophilic), hydrocortisone (moderately hydrophilic), ketoprofen (in neutral and deprotonated states), progesterone (hydrophobic and poorly water soluble) and danazol (hydrophobic and very poorly soluble). The structures of these drugs are shown in Fig. 1 and their physicochemical properties are summarized in Table I.

METHODS

Software and Hardware

MD simulations were performed using GROMACS (21–23) version 4.5.5 on facilities provided by Victorian Life Sciences Computation Initiative (VLSCI). The VLSCI hardware utilised was an SGI Altix XE Cluster of 1088 Intel Nehalem cores running at 2.66GHz connected with a QDR Voltaire Fabric InfiniBand network. The CPU time required for 100 ns of simulation time varied from 500 CPU hours for the 0% $^{w}/_{w}$ water systems to 21000 CPU hours for the 75%

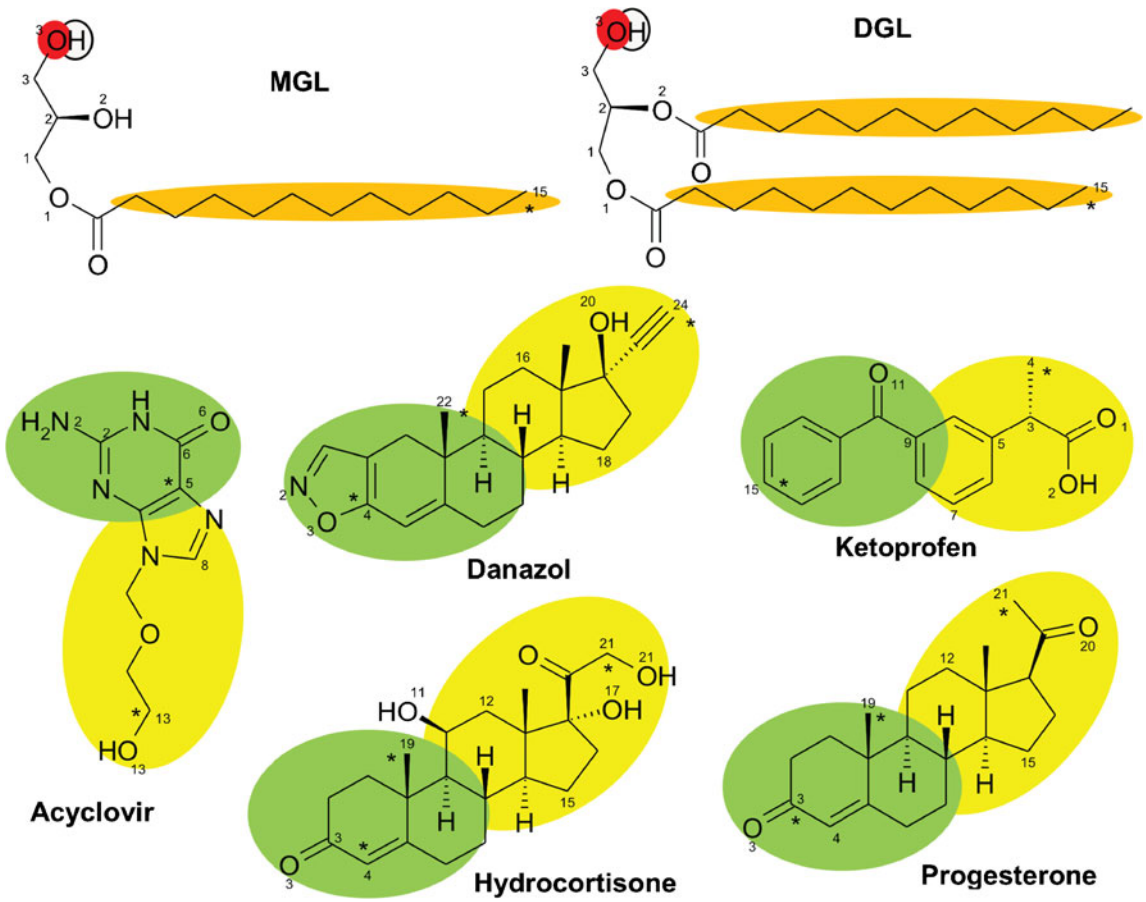

Fig. 1 Structures of the lipids mono-lauroyl glyceride (MGL) and di-lauroyl glyceride (DGL) used in the model Type I lipid formulation and the drugs; acyclovir, danazol, hydrocortisone, ketoprofen and progesterone. The molecule numbering used is indicated. Molecule coloring is to assist visualization of molecular orientation in Fig. 5. *Asterisks* denote reference atoms used for the calculation of the spatial distribution functions shown in Fig. 6.

$^{w}/_{w}$ water system. The total computation time required for the simulations presented was approximately 45,000 CPU hours. Visualisation of the simulation trajectories was performed using VMD (24). MD trajectories were analyzed using programs distributed as part of the GROMACS software package. Atom spatial distributions around drug molecules were calculated using g_sdf (25), distributed with GROMACS 4.0.7, using a bin width of 0.09 nm and a cell size 8×8×8 nm. A spatial distribution function describes the three dimensional probability of finding a particle around a given reference, relative to that of evenly distributed particles, and is the three dimensional equivalent of a radial distribution function which is presented in one dimension (radius). The program g_sdf requires reference atoms in each drug molecule, around which the spatial distribution function is calculated; the atoms C2, C6 and C8 were used for acyclovir, C4, C16 and C18 for danazol, C3, C12 and C15 for hydrocortisone, C3, C5 and C9 for ketoprofen, and C3, C12 and C15 for progesterone (Fig. 1). Water (water-OW) and glyceride (MGL-C15) radial distribution functions (RDFs) were calculated using g_rdf with a bin width of 0.002 nm. RDFs were calculated for selected drug atoms (asterisked in Fig. 1) and numerically integrated over the volume from 0 nm to the first RDF minimum to obtain the water-OW or MGL-C15

Table I Physical Properties of the Drugs Investigated in this Work

	MW (g mol^{-1})	Melting point (°C)	Aqueous solubility (mg cm^{-3})	log P
Acyclovir	225.2	225 (10)	1.8 (11)	−1.57 (12)
Danazol	337.5	227 (13)	0.00058 (14)	3.93 (13)
Ketoprofen	254.3	94.5 (15)	0.24 (16)	3.12 (17)
Hydrocortisone	362.5	220 (10)	0.30 (18)	1.61 (19)
Progesterone	314.5	129 (10)	0.007 (20)	3.87 (19)

coordination numbers. Radii of the first RDF minima used to calculate the coordination numbers are listed in the Supplementary Material, Table S1. Self-diffusion coefficients were calculated with g_msd, which determines the mean square displacement of atoms or molecules from their initial positions, fits a straight line using the least squares method to the central 80% of the time data and computes the self-diffusion constant using the Einstein relationship (26).

Simulation Specifications

Simulations were performed using the GROMOS 43A2 united atom forcefield (27,28) and SPC water (29) with a 5 fs time step. The density of SPC water of 969.6 kg m^{-3} at 310 K observed in this study is in good agreement with the expected value for water based on the SPC model @ 310 K of 970 kg m^{-3} (30). The larger simulation step size was obtained by increasing the mass of the polar hydrogens within the molecules to 4 Da and decreasing the attached heavy atom's mass by the same amount to conserve mass (31), a common technique for increasing the time step possible for a system (1,32–39). Changing the mass distribution in this manner decreases the vibration frequency of the hydrogen – heavy atom bond, allowing the use of a larger time step. The maximum time step in MD simulations is limited by the largest vibrational frequency found within the system (40). Changing the atomic masses in this manner does not influence the thermodynamic properties or dihedral angle distributions (31), and has been demonstrated to not affect the equilibrium properties of phospholipid bilayers (41). This mass redistribution between polar hydrogens and attached heavy atoms does not significantly alter the dynamic motion of molecules, as established by the constancy of self diffusion coefficients under different time steps and mass distributions (see Supplementary Information, Table S2). The water molecule geometry was constrained using SETTLE (42) and the remaining bond lengths were constrained with the LINCS algorithm (43). Periodic boundary conditions were employed on the initially cubic simulation cell, which is the classical manner to minimise edge effects in a finite system. The system being simulated is surrounded by translated copies of itself, producing an infinite repeating system without any liquid/vacuum boundaries. Electrostatic interactions were treated with a short range cut-off distance of 0.9 nm, with the long range electrostatic interactions then calculated using particle-mesh Ewald (PME, fourier grid spacing=0.12, interpolation order=4, relative strength of Ewald-shifted direct potential 1×10^{-5})(44). Lennard-Jones non-bonding interactions, i.e. van der Waals interactions, had a 0.9 nm cut-off with long range dispersion corrections for energy and pressure applied. The isothermal-isobaric or NPT ensemble was used, which refers to a system having a constant number of particles, pressure and temperature, with the velocity rescaling temperature coupling (45) (T_{ref}=310 K, τ_T=0.1 ps) and Parrinello-Rahman pressure coupling (46,47) (anisotropic, P_{ref}=1 atm, τ_P=2 ps). Temperature and pressure coupling are discussed further below.

To avoid biasing the phases formed during the simulation and the location that the drug molecules take within the system, the initial system geometries were generated by randomly placing molecules within the simulation cell using the script random_box from the Silico package (http://silico.sourceforge.net). This approach was utilised to ensure that spontaneous organisation of the phases and location of the drug molecules within these phases, and not based on the preconceived structures thought to be present. Initial phase organisation happens predominately within the first 20 ns, therefore the time taken to perform the simulations is not significant relative to the total simulation times performed.. Steepest decent energy minimisation[29] was used to remove bad van der Waals contacts between atoms, followed by three short 20 ps simulations to stabilize the system. The first short simulation was performed with Berensden temperature coupling (29) (τ_T=0.01 ps with reference temperature of 310 K) and no pressure coupling, the second with velocity rescaling temperature coupling (τ_T=0.1 ps) and anisotropic Berensden pressure coupling (29) (τ_P=4.0 ps with reference pressure of 1 bar and 4.5×10^{-5} compressibility in the x, y and z directions), and the third with anisotropic pressure coupling changed to Parrinello-Rahman (P_{ref}=1 atm, τ_P= 2 ps). The output from this final step was then used to commence the production runs. The bulk system properties, i.e. total energy and density, change rapidly over the first 5 ns and then alter more slowly as the system undergoes slower reorganization of the phase structure, as shown in the Supplementary Material Figure S1. After 50 to 80 ns these system properties stabilize and oscillate around an average value. Simulations were run for a minimum total simulation time of 100 ns. Ketoprofen, which is available as a racemic mixture of the R- and S- enantiomers, was modelled as the biologically active S-enantiomer (15).

Temperature Coupling

Temperature coupling is used in constant temperature molecular dynamics simulations to prevent drift in the system energy caused by force truncation and integration errors; with the latter becoming a significant issue at larger time steps. Constant temperature is achieved by coupling the particles to an external heat batch of a given temperature, which adds or removes heat from the system by scaling the atomic velocities. Temperature coupling must be used with care as it can introduce artifacts; for example the "flying ice cube", where thermal motion is transferred into a net center of mass velocity (48–50). It has also been previously noted that the energy exchange between different components of a simulated system is not perfect, and this can manifest as the solvent heating up while the solute cools (29,40,51). Therefore, the selection of

the appropriate temperature coupling algorithm and coupling groups (i.e. groups of atoms independently coupled to separated heat baths) is important to enable correct thermal behavior of the molecular species present.

Without careful attention, the 5 fs time step used in this study was observed to cause temperature differences between different phase regions. In a test phase separating system consisting of water, MGL and DGL (24,605, 600 and 600 molecules, respectively) with all molecules grouped together within a single temperature coupling group, although the overall system average was correct at 310 K, the temperature of the water molecules was about 30 K higher than that of the glycerides. This heat distribution artifact was addressed by separating the system into two separate temperature coupling groups; water and non-water (MGL + DGL) which resulted in all three molecule types being correctly maintained close to the reference temperature of the heat baths.

A complication with using this separation into water and non-water is how to handle the situation where a small number of drug molecules are introduced. The problem that arises is that there are insufficient numbers of the molecules to be coupled as a group in their own right to a heat bath and the molecules may interact with water only, glycerides only, or both. For simplicity, the drug molecules were grouped with the glycerides, which maintained the temperatures of all molecule types close to the reference temperature. For any phase separated system, it is recommended that close attention be paid to the application of temperature coupling to avoid temperature artifacts.

Pressure Coupling

Pressure coupling is used in constant pressure MD simulations to maintain the pressure at a target value. It works in a similar manner to temperature coupling, with the system pressure coupled to a "pressure bath", and particle coordinates and box dimensions scaled to adjust the pressure. The isothermal-isobaric (NPT) ensemble allows the selection of isotropic, semi-isotropic and anisotropic pressure coupling for pressure control. The most commonly used method is isotropic coupling; where the pressure is regulated by scaling inter-atomic distances (and correspondingly the cell dimensions) evenly among all three axes. Therefore, the cell is maintained at the same relative dimensions; i.e. if it starts as a cube then it will always remain a cube. In the current simulations anisotropic pressure coupling, in which the three cell dimensions are scaled independently, was chosen to ensure that the equilibrium structure reached by the formulations were not constrained or limited by the shape of the simulation cell. Due to the nature of periodic boundary conditions, structures that evolve must have an integer number of repeating units across the cell (33), and the selection of anisotropic pressure coupling reduces the influence this limitation has on the structures that evolve.

In the case of spontaneous aggregation of a phospholipid, isotropic pressure coupling has been demonstrated to influence the phases and molecular structures that can form (52). These authors observed that anisotropic coupling allowed the formation of a bilayer, whereas isotropic coupling forced the system to form unrealistic cylindrical micelles. Anisotropic pressure coupling has been shown to not influence the properties of phospholipid bilayers (41). A drawback of using anisotropic pressure coupling is that, under some conditions, a severe distortion of the simulation cell occurs where the cell becomes very short in one dimension occurs, leading to the simulation crashing. The driving force for this distortion appears to be a combination of the electric dipole moment and the surface tension of the interfaces between the two phases. The influence of the electric dipole moment can be clearly demonstrated by calculating the energies of an ion pair (Na^+/Cl^-) within cells of different dimensions, but having the same total volume (see Supplementary Material, Table S3). Cell dimensions that result in a closer association between the ion dipole and its periodic image have lower system energy thus driving a fully flexible cell to become shorter in one dimension. Failure of the anisotropic pressure coupled system was not encountered in this study due to the significantly lower calculated dipole moment (~2.3) compared to those of systems that have been observed to fail consistently (~30, personal observations within a sodium oleate/sodium laurate/water system (33)). It is also expected that the effect will diminish with increasing cell size.

RESULTS AND DISCUSSION

Phase Behavior of a Type I Formulation

In the first component of this work, we investigated the behavior of the MGL/DGL lipid formulation in the presence of different quantities of water, modelling the behavior of the formulation upon dispersion in an aqueous phase. A 1:1 mole ratio MGL/DGL formulation was simulated at ten different dilutions ranging from 0 to 75% $^{w}/_{w}$ water (100 to 25% $^{w}/_{w}$ total glyceride). Each simulation was between 100 and 200 ns. Systems were constructed using a constant number of MGL and DGL molecules, so the total system size varied between 32,000 atoms and 250,000 atoms, depending on the water content. The specifications of the formulation/water simulations are presented in Table II.

All of the model systems spontaneously organized with micellar structures forming at low water concentrations and phase separated systems at higher water concentrations. The structures formed are shown in Fig. 2 in order of increasing water concentration. These structures are consistent with our previous results (1) which were obtained using fewer and

Table II Specifications for Simulations of MGL/DGL Formulation Investigating the Influence of Water Content on the Formulation Phase Behavior

Water Content (% $^{w}/_{w}$)	[Water]/[GL]	MGL			DGL			Water		
		Number of molecules	Concentration		Number of molecules	Concentration		Number of molecules	Concentration	
	ω_0		% $^{w}/_{w}$	mol%		% $^{w}/_{w}$	mol%		% $^{w}/_{w}$	mol%
0	0	600	37.5	50.0	600	62.5	50.0	0	0	0
1	0.2	600	37.2	41.5	600	61.8	41.5	246	1.0	17.0
5	1.1	600	35.7	24.2	600	59.3	24.2	1,283	5.0	51.6
10	2.3	600	33.8	15.4	600	56.2	15.4	2,708	10.0	69.2
15	3.6	600	31.9	10.9	600	53.1	10.9	4,301	15.0	78.2
20	5.1	600	30.0	8.2	600	50.0	8.2	6,093	20.0	83.6
30	8.7	600	26.3	5.2	600	43.7	5.2	10,444	30.0	89.6
40	13.5	600	22.5	3.4	600	37.5	3.4	16,247	60.0	93.2
50	20.5	600	18.7	2.3	600	31.1	2.3	24,605	50.2	95.4
75	60.9	600	9.4	0.8	600	15.6	0.8	73,110	75.0	98.4
100	–	0	0	0	0	0	0	17,131	100	100

shorter simulations and covered a narrower concentration range. The previous work also used less accurate coupling algorithms and a simpler electrostatic treatment. In the system containing only glyceride, the hydroxyl functional groups of the glyceride molecules interact with each other through hydrogen bonding, forming a three dimensional network of reverse micelle-like channels containing the head groups surrounded by the alkane chains. As water is introduced, the glycerides aggregate into discrete reverse micelles formed around pools of water, maintaining the interactions between the hydrophilic hydroxyl functional groups of the glycerides and water. At 1% $^{w}/_{w}$ water, more than half of the reverse micellar structures contain no water molecules. The remaining reverse micellar structures contain one to three water molecules. When the amount of water present is increased to 5% $^{w}/_{w,}$ a dramatic change in the structure is observed. Distinct pools of water form and the majority of the glyceride headgroups make interactions with water. At 10 to 15% $^{w}/_{w}$ water, the dimensions of the water pools further increase while maintaining the reverse micellar structure. The next step, to 20% $^{w}/_{w}$ water, facilitates a further significant change in the structure, transforming the system from discrete water pools within the reverse micellar structure to one where the glyceride form a lamellar structure and the water forms large, continuous pools. This indicates that between 15 and 20% $^{w}/_{w}$ water, a phase transition occurs from a reverse micellar system to a phase separated water–oil system. This change is also made evident through a sharp increase in the fraction of alkane chain dihedrals that are present in the trans confirmation (Supplementary Material, Figure S2). Because the lamellar structures span the simulation cell it is expected that these lamellar structures do not precisely represent the nature of these phases in bulk systems - there is simply insufficient space for complete phase separation to occur and for the structures to form freely - but do reflect the general structure of the phase(s) present in this region i.e. a lamellar oily phase and bulk water. These limitations could be reduced by substantially increasing the simulation size, but this is currently not feasible at an atomistic level.

This analysis of molecular structure reveals three distinct phase regions; at low water content, bulk glyceride forms reverse micelle-like channels; a reverse micellar single phase occurs between 5 and 15% $^{w}/_{w}$ water and a phase separated water–oil system exists at high water concentrations. In subsequent figures these phase regions are respectively colored red, green and blue.

The density of the model systems (see Supplementary Material Section S1) decreases linearly from 0 to 15% $^{w}/_{w}$ water. Between 15 and 20% the system density increases due ordering of the glyceride tails in the phase separated system. The density of the model system was compared to the the commercial product Imwitor 308 which has >80% monoglyceride and a shorter C8 fatty acid. At low water concentrations both systems behaved similarly. Between 20 and 25% $^{w}/_{w}$ water, the density of the Imwitor 308 system decreases sharply, corresponding to the change from a continuous oil or reverse micellar phase to a phase separated system consistent with the experimental system having a shorter alkyl chain length and higher monoglyceride content. The model system density in the absence of water, 1,011.3 kg m^{-3}, is close to that determined experimentally for Imwitor 308, 1011.5 kg m^{-3}. The differences in the modelled and experimental systems can be attributed to Imwitor 308 having a shorter fatty acid chain and a high monoglyceride content.

The modeled phase behavior of this mixture of C12 straight chain fatty acid glycerides is consistent with

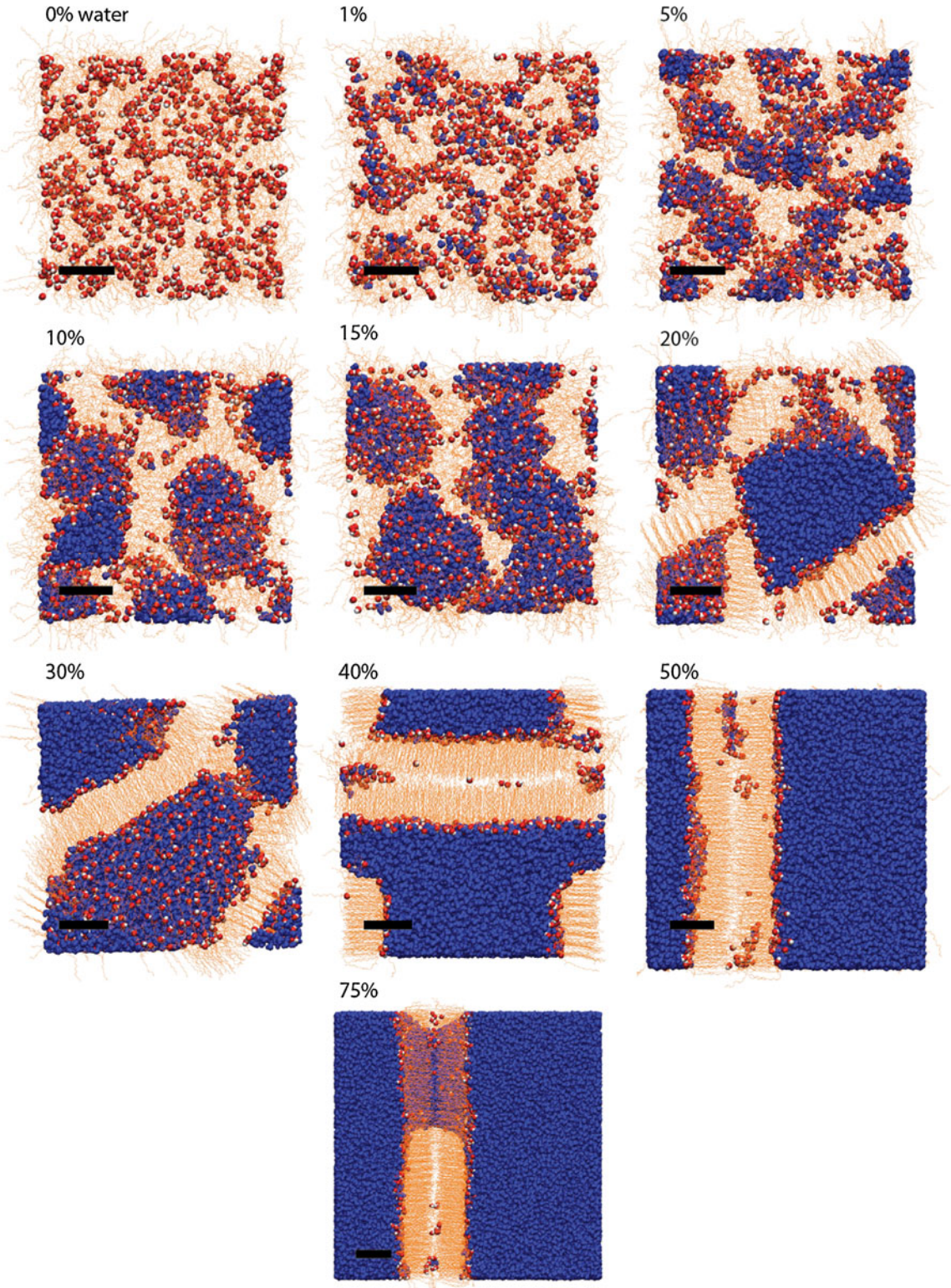

Fig. 2 Phases formed in simulations of the Type I MGL/DGL lipid formulation as it is diluted in water. 0–1% $^{w}/_{w}$ water give a reverse micelle-like phase containing isolated water molecules. 5–15% $^{w}/_{w}$ water forms a reverse micelle phase containing discrete water pools; 20–75% $^{w}/_{w}$ water forms separated water and lamellar phases. Water molecules are *blue*, the O3 and H3 atoms of MGL and DGL are *red* and *white* respectively, and the alkane chains of the glycerides are *orange*. Note that although the simulation systems differ in size, the images are scaled to a uniform size. A scale bar 2 nm in length is shown on each system.

experimental observations of similar mono- and di-glycerides. The monoglycerides of lauric acid (C12, saturated, as used in this study), palmitic acid (C16, saturated) and stearic acid (C18, saturated) do not disperse in water by themselves but do undergo some swelling with water into a gel phase (53,54). Additionally, it has been observed that the monoglycerides only form an L_2 phase or lytroropic liquid crystal phase with excess water, i.e. capric acid monoglyceride (C10, saturated) (55). A single component system of monoolein (octadecenoic monoglyceride, C18 fatty acid with a cis double bond in the C9 position) forms a lamellar phase at less than 10% $^{w}/_{w}$ water, then a cubic phase up to 40% $^{w}/_{w}$ water (56). Mixtures of oleic acid glycerides (C18 unsaturated, with a cis double bond at C9) form micellar and lamellar phases at high water concentrations, and a cubic phase with high monoglyceride content in the region of 50 to 80% $^{w}/_{w}$ water (57). The commercial grade products of Imwitor 308 and Imwitor 988 (C8 chain length, 47 to 57% monoglyceride, remainder di- and triglycerides) have been found to absorb 20 and 14% $^{w}/_{w}$ at 37°C, respectively, before undergoing phase separation (9).

Hydration of Glyceride Head Groups

The complex phase behavior of lipid systems is controlled by a variety of factors – particularly by the energetics of head group solvation and packing of the hydrophobic tails. The water coordination number (i.e. the number of water molecules in the first solvation shell of a given atom) is a useful probe of the phase behavior. The radii of the first RDF minima used to calculate the coordination numbers are listed in the Supplementary Material, Table S1. Figure 3 shows the number of waters surrounding the hydroxyl groups of the glycerides (atom O3) and water oxygens (OW) plotted against water concentration. The most rapid change in coordination occurs within the low water reverse-micelle like phase region below 10% $^{w}/_{w}$ water (ω_0=2.3, where ω_0 is the ratio of water to glyceride concentration) and filling of the first solvation shell is essentially complete when the water content reaches 20–30% $^{w}/_{w}$ (ω_0=5.1–8.7). These results are consistent with experimental observations of shell and pool (core) water in reverse micelles (58). Figure 3 also shows that the coordination numbers for the 30% $^{w}/_{w}$ water simulation are slightly higher than would be consistent with the adjacent results. We attribute this minor variation to perturbation induced by the periodic cell. When the ratio of water to glyceride concentration (ω_0) is 2, this indicates that there is only shell water, all of the water molecules are associated with the surfactant head groups (58). This corresponds to approximately 10% $^{w}/_{w}$ water.

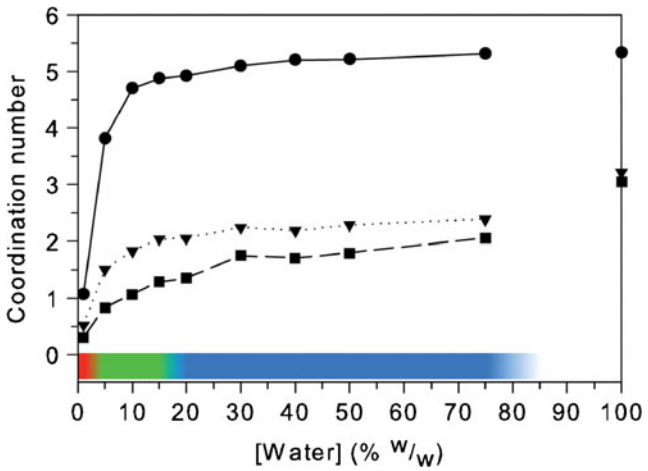

Fig. 3 Water coordination number of the first hydration shells of atoms MGL-O3 (▼), DGL-O3 (■) and water-OW (●) in the MGL/DGL formulation plotted against water concentration. The block color scale denotes the identified phase regions; isolated waters (*red*), reverse micellar (*green*) and separate water and lamellar phases (*blue*). The phase behavior of the 80–100% $^{w}/_{w}$ water region has not been fully investigated so the block color scale is omitted from this part of the plot.

Diffusion of Water and Glycerides

Phase changes often cause sharp changes in molecular mobility. The self-diffusion coefficients of water and glyceride molecules therefore provide useful information about the state of the system. Analysis of water self-diffusion shows that two separate diffusional processes are occurring; fast and slow (see Supplementary Material, Figure S4). The fast and slow self-diffusion coefficients of water in the MGL/DGL formulation are shown in Fig. 4a. The slow diffusion process can be attributed to water bound to lipid head groups, while the faster process is due to water molecules within the water pools diffusing more freely. The diffusion rate of the fast component increases rapidly between 15 and 20% $^{w}/_{w}$ water, coinciding with the phase transition from reverse micelle to separated phases containing large water pools. The slow diffusion component increases more slowly as the amount of bulk water in the system increases. For the MGL:DGL system in the reverse micelle phase we obtain values for the slow component of water diffusion between 0.0025×10^{-5} cm^2s^{-1} and 0.04×10^{-5} cm^2s^{-1} (Fig. 4b). Experimental measurements of the slow component of water diffusion have been made in a glyceryl monooleate cubic phase (81% water, Ia3d phase) (59), giving a value of 0.03×10^{-5} cm^2s^{-1}. Although these systems differ in chemical composition and structure, both systems contain constrained pools of water surrounded by glyceride head groups and the simulation results appear to be generally consistent with the experimental values. The SPC model of water is known to overestimate the bulk water diffusion coefficient by ~60%, 3.9×10^{-5} cm^2 s^{-1} (60) *versus* 2.3×10^{-5} cm^2 s^{-1} (61) at 25°C, and the value of 4.3×10^{-5} cm^2 s^{-1} at 37°C determined in this study is consistent with previous observations.

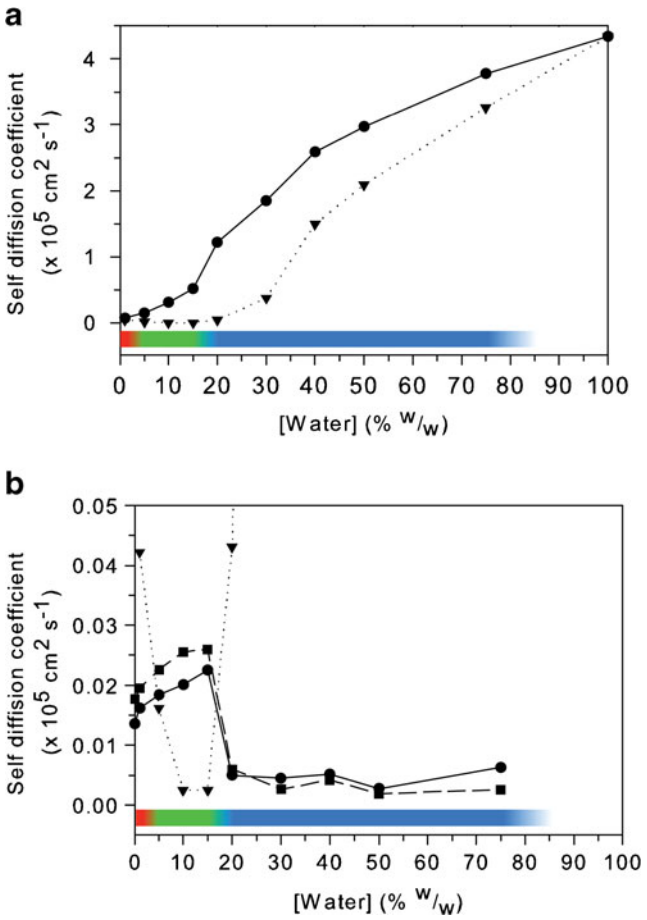

Fig. 4 The self-diffusion coefficients of water and glyceride molecules in MGL/DGL formulations. (**a**) Water fast diffusion (●, fitted over Δt 0.1 to 0.9 ns) and slow diffusion (▼, fitted over Δt 1 to 9 ns). (**b**) Glyceride self-diffusion coefficients, MGL (●) and DGL (■). Part of the water slow diffusion curve is also shown (▼). The block color scale denotes the identified phase regions as for Fig. 3.

The self-diffusion coefficients of the glycerides behave in a distinctly different manner from water and are shown in Fig. 4b. The first introduction of water into the formulation, moving from 0 to 1% $^{w}/_{w}$ water, allows the glyceride molecules to move more freely and the self-diffusion coefficients of both glycerides increases until 15% $^{w}/_{w}$ water is reached. Beyond this point, the glycerides form a lamellar phase and therefore become more constrained in their available motions, sharply reducing the diffusion coefficients. The diffusion coefficients of glycerol monooleate have been measured within cubic phases as 0.018×10^{-5} cm^2s^{-1} (Ia3d cubic phase, 22% water) (62), 0.024×10^{-5} cm^2s^{-1} (Pn3m cubic phase, 39.5% water) (62) and 0.02×10^{-5} cm^2s^{-1} (Ia3d cubic phase, 81% water) (59). The diffusion coefficients in the mixed glyceride simulations are lower than observed for the glycerol monooleate at similar water concentrations; MGL=0.005/DGL=0.006 and MGL=0.005/DGL=0.004×10^{-5} cm^2s^{-1} at 20 and 40% $^{w}/_{w}$ water, respectively. It would be expected that the diglyceride would both increase the viscosity of the system and diffuse more slowly than the pure monoglyceride. The diffusion coefficients within the reverse micelle region ($0.016–0.026\times10^{-5}$ cm^2s^{-1}) are comparable those measured in the glycerol monooleate cubic phase.

Drug Dispersion and Dynamics Within the Type I Formulation

To investigate the behavior of drugs within the Type I formulation as it is diluted with water, we executed 100 ns MD simulations of the six model drugs (acyclovir, danazol, hydrocortisone, ketoprofen in neutral and deprotonated forms, and progesterone) in lipid formulations containing 1, 10, 20 and 50% $^{w}/_{w}$ water starting in each case from random molecular mixtures as described above. In each simulation system, 18 drug molecules were combined with 600 molecules each of MGL and DGL (1:1 molar ratio) and between 245 and 24,605 water molecules (Tables II and III). The loading of 18 drug molecules was selected to be of the same order of magnitude as found within existing lipid formulations, and to avoid the issue of significant drug-drug interactions present at higher loadings. This number of drug molecules within the system equates to the following drug loadings of 9, 9, 14, 10 and 15 mg ml^{-1}, for acyclovir, danazol, ketoprofen, hydrocortisone, and progesterone, respectively, within the pure MGL:DGL formulation. In all, 24 simulations were performed.

To investigate the dispersion of drug molecules and their dynamic behavior within the formulation/water mixtures we analyzed the localization of drug molecules within the formulation, drug intermolecular interactions and drug diffusion properties. Figure 5 shows the locations of drug molecules within the diluted MGL/DGL formulations at the completion of each 100 ns simulation. To highlight the orientation of the molecules they are colored yellow and green using the color scheme shown in Fig. 1. To visualize the time-averaged interactions of the drugs with the aqueous and lipid regions of the

Table III Specifications for the Six Sets of Four Simulations Investigating the Influence of Glyceride Content on Drug Behavior in the MGL/DGL Lipid Formulation. Each Set of Four Simulations Contained One of the Model Drugs; Acyclovir, Danazol, Hydrocortisone, Neutral Ketoprofen, Deprotonated Ketoprofen or Progesterone

Water (% $^{w}/_{w}$)	Glyceride (% $^{w}/_{w}$)	Number of molecules			
		Drug	MGL	DGL	Water
1	99	18	600	600	246
10	90	18	600	600	2,708
20	80	18	600	600	6,093
50	50	18	600	600	24,605

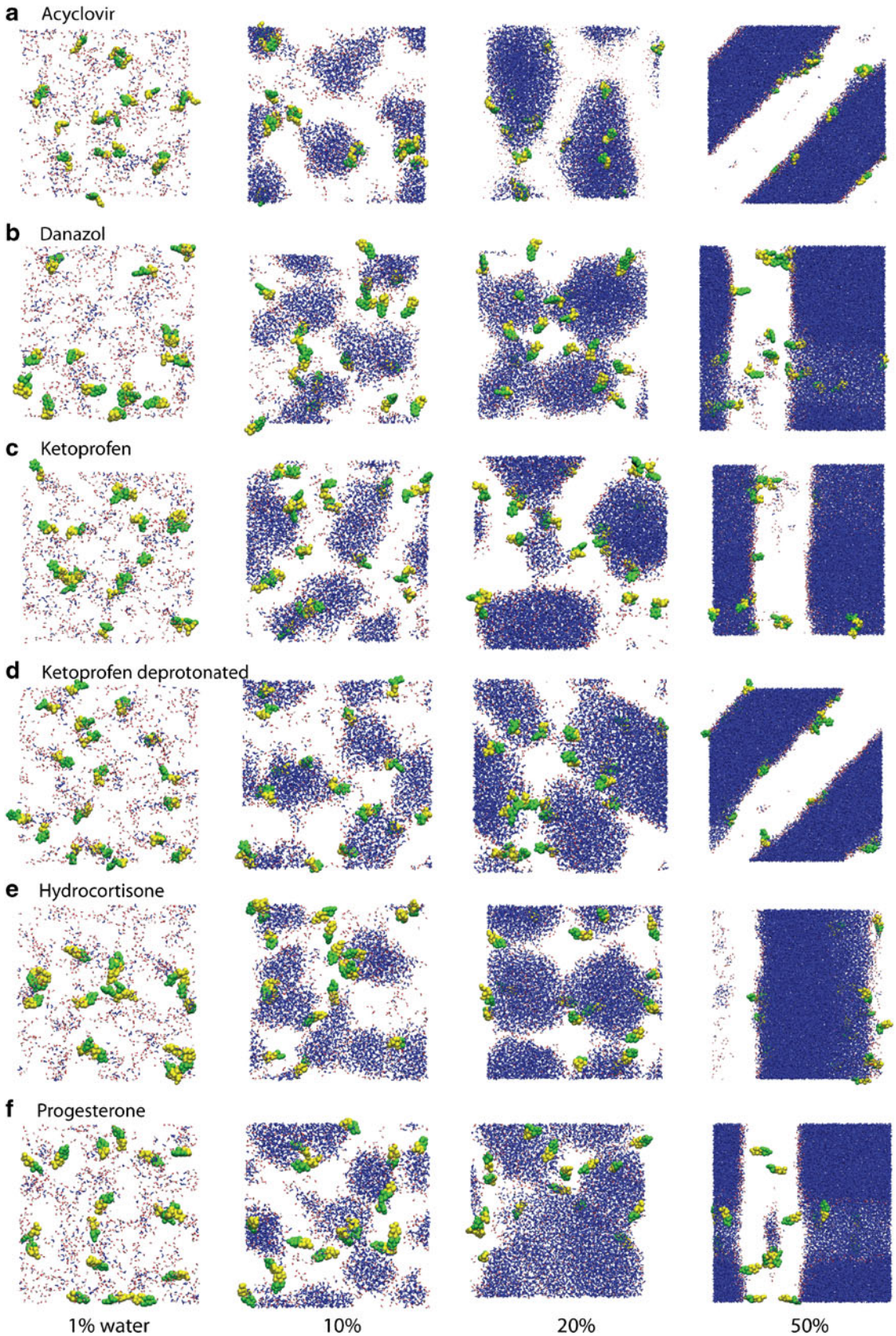

Fig. 5 Localization of drugs within the final frames of the MGL/DGL formulation simulations with changing glyceride concentration. Drug molecules are colored *green* and *yellow* as illustrated in Fig. 2. Water is *blue*. MGL/DGL oxygen atoms are *red* and carbon atoms are not shown.

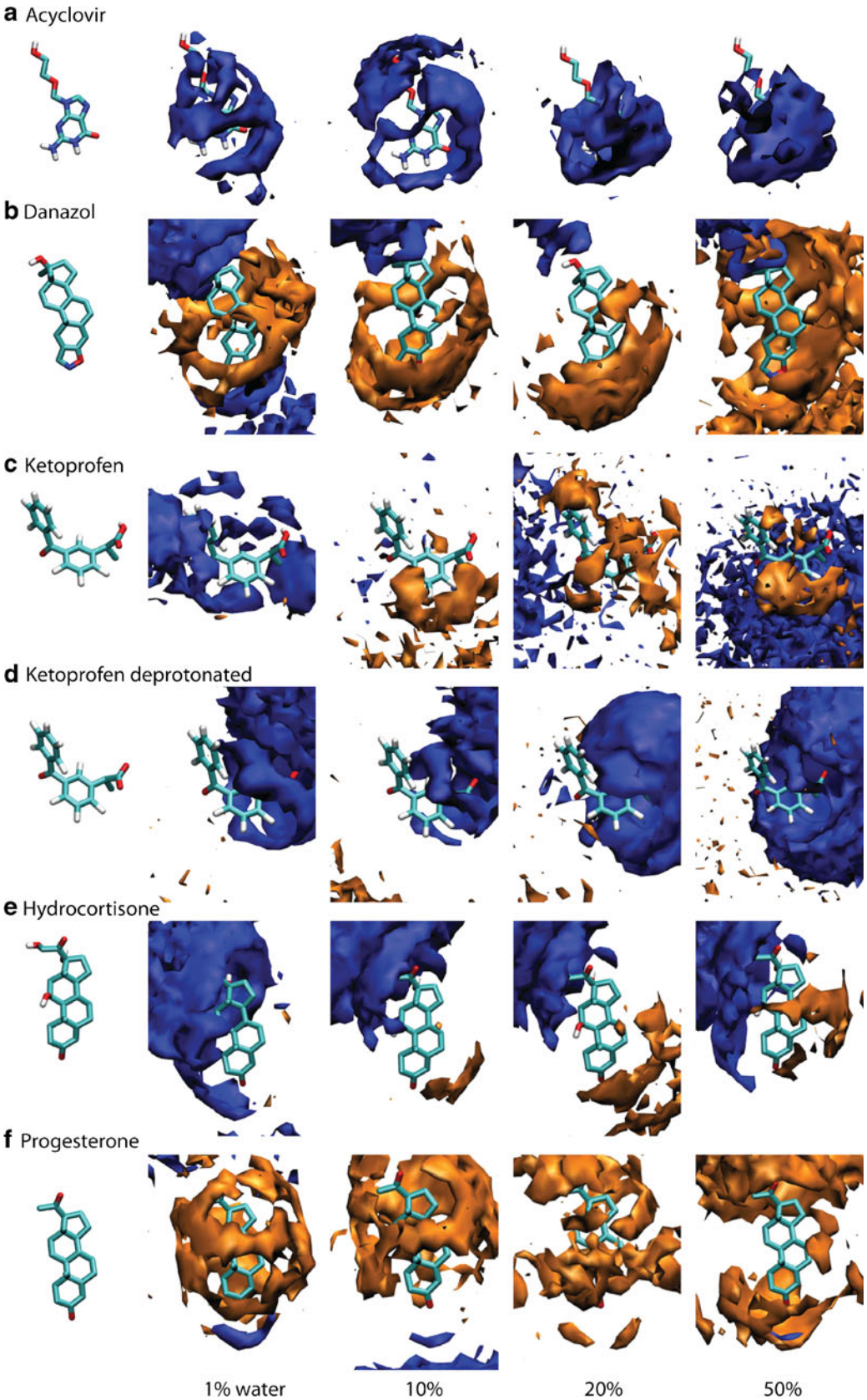

Fig. 6 Spatial distribution functions of water-OW (*blue*) and MGL-C15 (*orange*) atoms around drugs in the MGL/DGL formulations. Drug molecules alone are shown on the left to indicate the molecule's orientation. Probabilities used to generate the surfaces are listed in Supplementary Material Table S4.

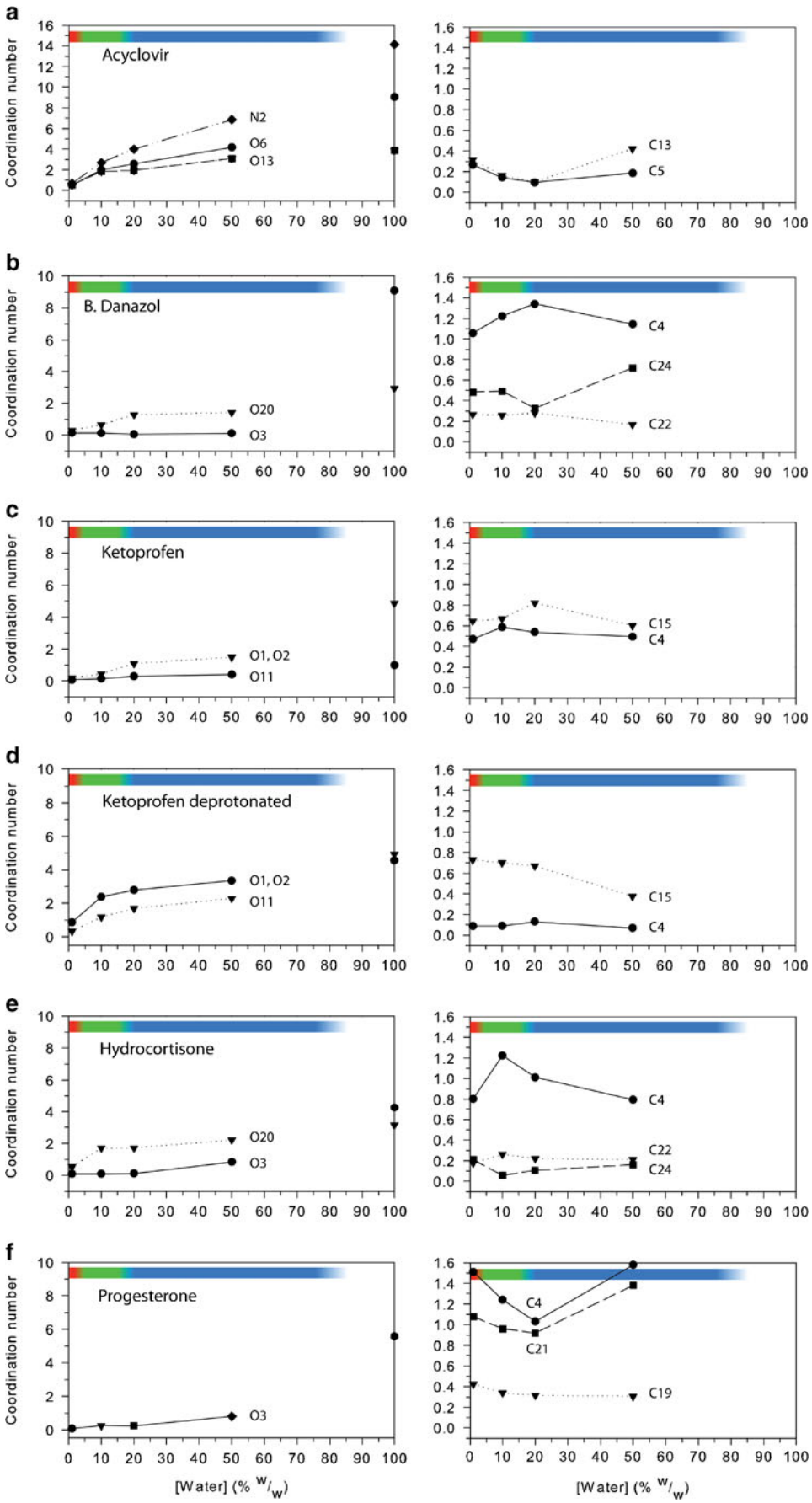

Fig. 7 Water OW (LHS) and lipid MGL-C15 (RHS) coordination numbers for selected drug atoms plotted as a function of water concentration. Atom names are shown in Fig. 1. Radii used to calculate coordination numbers are shown in Supplementary Material Table S1. The block color scale identifies the phase regions described in the caption for Fig. 3.

formulations, we calculated the spatial distribution of water oxygen atoms (OW) and with the terminal atom of the monoglyceride hydrophobic tail (MGL-C15) around each of the drugs, which are shown in Fig. 6. The probabilities used to generate the isosurfaces are given in Supplementary Material, Table S4. To quantitfy changes in the solvation of the drugs with changes in water content of the formulation we calculated coordination numbers for selected drug atoms (Fig. 7), which were generated using solvation shell radii reported in Supplementary Material Table S1.

Acyclovir was chosen as an example of a hydrophilic drug with modest aqueous solubility and is the most polar of the drugs investigated. The final structures of the acyclovir/formulation mixtures (Fig. 5a) show that in all simulations the acyclovir molecules locate within the aqueous phase, although they do not reside within the bulk water regions, but are instead associated with the lipid/water interface where they make interactions with the lipid head groups. At the higher water concentrations they also make pairing interactions with other acyclovir molecules. Some acyclovir dimers are evident in the simulation of formulation containing 10% water, and at 20 and 50% significant stacking of the molecules occurs. The spatial distribution functions for acyclovir (Fig. 6a) show that at all water concentrations the drug interacts strongly with water through the amino and carbonyl groups (N1, N2 and O6). The plots of coordination number (Fig. 7a) show that acyclovir becomes rapidly solvated as the water content of the formulation is increased and that the O13 hydroxyl group, in particular, is nearly maximally solvated at 10% $^{w}/_{w}$ water concentration. The interaction between acyclovir atoms and MGC-C15 is very low in all simulations. This observed behavior is consistent with the hydrophilic nature of acyclovir (logP = −1.57) and the reason for its low aqueous solubility is demonstrated by the easy stacking that occurs between the molecules.

Danazol is a highly lipophilic compound (logP = 3.93) with an extremely low aqueous solubility that has been widely investigated as a model compound for the study of lipid-based drug formulations (63–66). The final simulation frames (Fig. 5b) clearly show that the danazol molecules reside within the alkane-chain region of the dispersed formulations at all water concentrations. At lower water concentrations, when the formulation has a more disordered structure, the hydrophilic nature of both ends of the molecule can be satisfied by the molecule spanning the alkane region from one aqueous region to a neighboring, which is evident in the spatial distribution function of the 1% water concentration (Fig. 6b). At the 50% water concentration the formulation changes phase to form a lamellar system and the danazol molecular align with the bilayer, making contact with water only through O20. The atom coordination numbers (Fig. 7b) provide a consistent picture, with low water coordination numbers and relatively high coordination numbers for MGL-C15.

Ketoprofen was modeled in ionized (with a sodium counter ion) and neutral forms. In both forms, the molecules localize to the water/lipid interface (Figs. 5c and d) with the carboxylic acid or carboxylate (O1-2) and ketone groups (O11) projecting into the water and the hydrophobic aromatic rings residing within the glyceride. The spatial distribution functions (Figs. 6c and d) show that the deprotonated form is solvated much more strongly by water. Some aggregation of the neutral ketoprofen molecules occurs at water concentrations above 1% $^{w}/_{w}$, with preference for interaction through the formation of a carboxylic acid dimer. The water coordination numbers (Figs. 7c and d) show the relatively low aqueous solvation of the deprotonated form and a high degree of solvation of the deprotonated form.

The arrangement of the less lipophilic steroid hydrocortisone (logP = 1.61) within the formulations is shown in Fig. 5e. Due to the presence of three hydroxy groups, the side-chain and steroid C and D rings interact preferentially with the water pools, while the A and B rings are directed into the glyceride alkane chain region. In some instances at low water concentrations, the molecules span the region between reverse micellar water pools, as observed for danazol.

Finally, progesterone, like danazol, is poorly water soluble with a high logP (3.87). Progesterone does not contain any hydrogen bond donating groups (e.g. alcohols) and is most frequently found buried deeply within the lipid region (Figs. 6 and 7f). The ketone oxygen atoms (O3 and O20) do make interactions with water, although this interaction is not strong. No sustained aggregation of the progesterone molecules was observed.

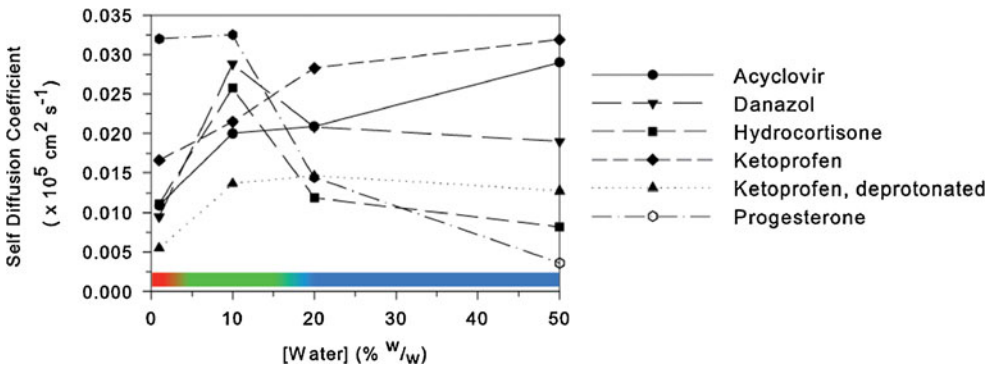

Fig. 8 Effect of water concentration on the self-diffusion coefficient of drugs within the MGL/DGL formulation. The block color scale identifies the phase regions described in the caption for Fig. 3.

Self-diffusion coefficients calculated for the drugs in each of the formulation/water mixtures are plotted Fig. 8. The curves can be classified into two groups; the more polar compounds which maintain their mobility when the formulation is diluted (acyclovir and both forms of ketoprofen) and the hydrophobic compounds, which become less mobile upon dilution of the formulation (danazol, hydrocortisone and progesterone). Members of the first group reside within the aqueous compartments of the system, which become larger as the water content increases and they therefore able to diffuse more easily at higher water content. The deprotonated form of ketoprofen has a much lower mobility than the protonated form in all of the simulations which is attributable to an increased interaction strength between the carboxylate acid group and the glyceride head groups (Supplementary Material Figure S5) and also with water. The second group of more hydrophobic compounds are more localized to the lipid phase and exhibit a diffusion maximum in the reverse micelle phase where there is greatest mobility of the lipids themselves (see Fig. 4b), followed by a sharp drop in mobility upon formation of the lipid lamellar phase. Among the compounds investigated, progesterone has the highest mobility in the isolated water phase because it does not contain any hydrogen bond donors and is more weakly associated with the water molecules present in the system.

CONCLUSIONS

The dissolution of drugs within lipid formulations and the dispersion of the formulation and drug within the aqueous medium of the gastrointestinal lumen the drug are important processes that determine the ultimate absorption or non-absorption of a formulated drug. However, these processes are currently poorly understood. In this work we have developed improved MD methods that provide an atomic-scale model of drug dispersion and dynamics and provide the first simulations of drugs within a lipid formulation.

Simulations of model Type I formulation/water mixtures reveal three distinct phase regions in the range 0 to 75% $^{w}/_{w}$ water; a single reverse micelle-like phase containing isolated water molecules at low water content, a single reverse micelle phase at intermediate water content and, at high water content, a two phase system consisting of lamellar glyceride and bulk water pools.

Simulations of the poorly water soluble drugs, acyclovir, danazol, hydrocortisone, ketoprofen and progesterone within the formulation/water systems show that at all water concentrations the localization of the drugs is driven by the local polar/non-polar or hydrophobic/hydrophilic properties of the drug itself. Drugs localize within the system in a way that best satisfies the formation of local hydrophobic or polar contacts with water, the formulation or with other drug molecules. Even polar drugs, such as acyclovir, contain hydrophobic regions or faces, and optimally make contacts with the lipid formulations. We therefore observe that acyclovir localizes to the lipid head group region, where the polar region of the drug is able to interact with water or polar lipid atoms while the less polar portion (the faces of the aromatic rings) can be shielded from water by interaction with the lipid. Similar behavior is observed for the other more polar drugs investigated; ketoprofen and hydrocortisone. The drugs containing fewer hydrogen bonding groups bind deeper within the alkane tail region of the lipids. Progesterone, which has only two hydrogen bond acceptor atoms, resides deep within the lipid region. Danazol, which is slightly more polar, having one hydrogen bond donor and three acceptors, also resides within the lipid but closer to the lipid/water interface where the hydroxyl group can make contact with water.

This development of MD models for lipid formulations provides important information about the localization within the formulation and dynamic processes such as aggregation that will result in poor solubilisation properties. It highlights the differences in physical behavior of different compounds. It provides a foundation for the *in silico* design of lipid formulations and towards this end we are currently extending this approach to consider a wider range of drugs, excipients and lipid formulations.

ACKNOWLEDGMENTS AND DISCLOSURES

Financial support from Capsugel is gratefully acknowledged. We would also like to thank the Victorian Life Sciences Computation Initiative (VLSCI) and the National Computational Infrastructure (NCI) for technical support and Merit Allocation Scheme grants of CPU time.

REFERENCES

1. Warren DB, Chalmers DK, Pouton CW. Structure and dynamics of glyceride lipid formulations, with propylene glycol and water. Mol Pharm. 2009;6(2):604–14.
2. Turner DC, Yin F, Kindt JT, Zhang H. Molecular dynamics simulations of glycocholate/oleic acid mixed micelle assembly. Langmuir. 2010;26(7):4687–92.
3. Bogusz S, Venable RM, Pastor RW. Molecular dynamics simulations of octyl glucoside micelles: structural properties. J Phys Chem B. 2000;104:5462–70.
4. Rane SS, Anderson BD. Molecular dynamics simulations of functional group effects on solvation thermodynamics of model solutes in decane and tricaprylin. Mol Pharm. 2008;5:1023–36.
5. Marrink SJ, Tieleman DP. Molecular dynamics simulation of a lipid diamond cubic phase. J Am Chem Soc. 2001;123(49):12383–91.
6. Kasimova AO, Pavan GM, Danani A, Mondon K, Cristiani A, Scapozza L, *et al*. Validation of a novel molecular dynamics simulation approach for lipophilic drug incorporation into polymer micelles. J Phys Chem B. 2012;116(14):4338–45.

7. Pouton CW. Lipid formulations for oral administration of drugs: non-emulsifying, self-emulsifying and 'self-microemulsifying' drug delivery systems. Eur J Pharm Sci. 2000;11:S93–8.
8. Pouton CW. Formulation of poorly water-soluble drugs for oral administration: physicochemical and physiological issues and the lipid formulation classification system. Eur J Pharm Sci. 2006;29(3–4):278–87.
9. Mohsin K, Pouton CW. The influence of the ratio of lipid to surfactant and the presence of cosolvent on phase behaviour during aqueous dilution of lipid-based drug delivery systems. J Drug Del Sci Tech. 2012;22(6):531–40.
10. CRC Handbook of Chemistry and Physics. Boca Raton, Florida: CRC Press/Taylor and Francis; 2010. Available from: http://www.hbcpnetbase.com.
11. Zielenkiewicz W, Golankiewicz B, Perlovich G, Koźbiał M. Aqueous solubilities, infinite dilution activity coefficients and octanol–water partition coefficients of tricyclic analogs of acyclovir. J Solution Chem. 1999;28(6):731–45.
12. Kristl A, Tukker JJ. Negative correlation of n-octanol/water partition coefficient and transport of some guanine derivatives through rat jejunum in vitro. Pharm Res. 1998;15(3):499–501.
13. Alsenz J, Meister E, Haenel E. Development of a partially automated solubility screening (PASS) assay for early drug development. J Pharm Sci. 2007;96(7):1748–62.
14. Erlich L, Yu D, Pallister DA, Levinson RS, Gole DG, Wilkinson PA, *et al*. Relative bioavailability of danazol in dogs from liquid-filled hard gelatin capsules. Int J Pharm. 1999;179(1):49–53.
15. Ying Hong Lu CBC. Physicochemical properties, binary and ternary phase diagrams of ketoprofen. Chirality. 2004;16(8):541–8.
16. Fujii M, Hori N, Shiozawa K, Wakabayashi K, Kawahara E, Matsumoto M. Effect of fatty acid Esters on permeation of ketoprofen through hairless rat skin. Int J Pharm. 2000;205(1–2):117–25.
17. La Rotonda MI, Amato G, Barbato F, Silipo C, Vittoria A. Relationships between octanol-water partition data, chromatographic indices and their dependence on pH in a set of nonsteroidal anti-inflammatory drugs. Quant Struct-Act Rel. 1983;2(4):168–73.
18. Hagen TA, Flynn GL. Solubility of hydrocortisone in organic and aqueous media: evidence for regular solution behavior in apolar solvents. J Pharm Sci. 1983;72(4):409–14.
19. Shoshtari SZ, Wen J, Alany RG. Octanol water partition coefficient determination for model steroids using an HPLC method. Lett Drugs Des Discov. 2008;5(6):394–400.
20. Nandi I, Bateson M, Bari M, Joshi HN. Synergistic effect of PEG-400 and cyclodextrin to enhance solubility of progesterone. AAPS PharmSciTech. 2003;4(1):E1.
21. Berendsen HJC, van der Spoel D, van Drunen R. GROMACS: a message-passing parallel molecular dynamics implementation. Comput Phys Commun. 1995;91(1–3):43–56.
22. Lindahl E, Hess B, van der Spoel D. GROMACS 3.0: a package for molecular simulation and trajectory analysis. J Mol Model. 2001;7:306–17.
23. van der Spoel D, van Buuren AR, Apol E, Meulenhoff PJ, Tieleman DP, Sijbers ALTM, *et al*. GROMACS user manual version 3.1.1. Groningen: Department of Biophysical Chemistry; 2002. p. 278.
24. Humphrey W, Dalke A, Schulten K. VMD: visual molecular dynamics. J Mol Graph. 1996;14(1):33–8.
25. Freudenberger C. g_sdf. 1.25 ed: Chemistry, University of Ulm; 2003.
26. Einstein A. The motion of elements suspended in static liquids as claimed in the molecular kinetic theory of heat. Ann Phys-Berlin. 1905;17(8):549–60. German.
27. van Gunsteren WF, Billeter SR, Eising AA, Hunenberger PH, Krueger P, Mark AE, *et al*. Biomolecular simulation: the GROMOS96 manual and user guide. Zurich: Hochschulverlag AG an der ETHC Zurich; 1996.
28. Daura X, Mark AE, Van Gunsteren WF. Parametrization of aliphatic CHn united atoms of GROMOS96 force field. J Comput Chem. 1998;19(5):535–47.
29. Berendsen HJC, Postma JPM, Gunsteren WF, Dinola A, Haak JR. Molecular dynamics with coupling to an external bath. J Chem Phys. 1984;81:3684–9.
30. Jorgensen WL, Jenson C. Temperature dependence of TIP3P, SPC, and TIP4P water from NPT Monte Carlo simulations: seeking temperatures of maximum density. J Comput Chem. 1998;19(10):1179–86.
31. Feenstra KA, Hess B, Berendsen HJC. Improving efficiency of large time-scale molecular dynamics simulations of hydrogen-rich systems. J Comput Chem. 1999;20(8):786–98.
32. Poger D, Mark AE. Lipid bilayers: the effect of force field on ordering and dynamics. J Chem Theory Comput. 2012;8(11):4807–17.
33. King DT, Warren DB, Pouton CW, Chalmers DK. Using molecular dynamics to study liquid phase behavior: simulations of the ternary sodium laurate/sodium oleate/water system. Langmuir. 2011;27(18):11381–93.
34. Paluch AS, Mobley DL, Maginn EJ. Small molecule solvation free energy: enhanced conformational sampling using expanded ensemble molecular dynamics simulation. J Chem Theory Comput. 2011;7(9):2910–8.
35. Anselmi M, Brunori M, Vallone B, Di Nola A. Molecular dynamics simulation of deoxy and carboxy murine neuroglobin in water. Biophys J. 2007;93(2):434–41.
36. Warren DB, Chalmers DK, Hutchison K, Dang W, Pouton CW. Molecular dynamics simulation of spontaneous bile salt aggregation. Colloids Surf A. 2006;280:182–93.
37. Tieleman DP, van der Spoel D, Berendsen HJC. Molecular dynamics simulations of dodecylphosphocholine micelles at three different aggregate sizes: micellar structure and chain relaxation. Biophys J. 2000;104:6380–8.
38. Marrink SJ, Mark AE. Molecular dynamics simulations of mixed micelles modelling human bile. Biochemistry. 2002;41:5375–82.
39. Bandyopadhyay S, Chanda J. Monolayer of monododecyl diethylene glycol surfactants adsorbed at the air/water interface: a molecular dynamics study. Langmuir. 2003;19:10443–8.
40. van der Spoel D, Lindahl E, Hess B, van Buuren AR, Apol E, Meulenhoff PJ, et al. GROMACS User Manual version 4.5.4 2010.
41. Anézo C, de Vries AH, Höltje H-D, Tieleman DP, Marrink S-J. Methodological issues in lipid bilayer simulations. J Phys Chem B. 2003;107(35):9424–33.
42. Miyamoto S, Kollman PA. SETTLE: an analytical version of the SHAKE and RATTLE algorithm for rigid water models. J Comput Chem. 1992;13:952–62.
43. Hess B, Bekker H, Berendsen HJC, Fraaije JGEM. LINCS: a linear constraint solver for molecular simulations. J Comput Chem. 1997;18:1463–72.
44. Essmann U, Perera L, Berkowitz ML, Darden T, Lee H, Pedersen LG. A smooth particle mesh ewald method. J Chem Phys. 1995;103(19):8577–93.
45. Bussi G, Donadio D, Parrinello M. Canonical sampling through velocity rescaling. J Chem Phys. 2007;126(1):014101.
46. Parrinello M, Rahman A. Polymorphic transitions in single-crystals - a new molecular-dynamics method. J Appl Phys. 1981;52(12):7182–90.
47. Nose S, Klein ML. Constant pressure molecular-dynamics for molecular-systems. Mol Phys. 1983;50(5):1055–76.
48. Harvey SC, Tan RKZ, Cheatham TE. The flying ice cube: velocity rescaling in molecular dynamics leads to violation of energy equipartition. J Comput Chem. 1998;19(7):726–40.
49. Chiu S-W, Clark M, Subramaniam S, Jakobsson E. Collective motion artifacts arising in long-duration molecular dynamics simulations. J Comput Chem. 2000;21(2):121–31.

50. Cheatham Iii TE, Brooks BR. Recent advances in molecular dynamics simulation towards the realistic representation of biomolecules in solution. Theor Chem Acc. 1998;99(5):279–88.
51. Lingenheil M, Denschlag R, Reichold R, Tavan P. The "Hot-solvent/cold-solute" problem revisited. J Chem Theory Comput. 2008;4(8):1293–306.
52. Patel RY, Balaji PV. Effect of the choice of the pressure coupling method on the spontaneous aggregation of DPPC molecules. J Phys Chem B. 2005;109(30):14667–74.
53. Larsson K, Krog N. Structural properties of the lipid—water gel phase. Chem Phys Lipids. 1973;10(2):177–80.
54. Kanesaka I, Shimizu K. Infrared intensity and morphology of 1-monolaurin–water systems. Spectrochim Acta A. 2000;56(3):523–9.
55. Ljusberg-Wahren H, Gunnarsson T, Wannerberger L, Gustafsson J, Almgren M, Krog N. Micelles and liquid crystals in aqueous diglycerol monodecanoate systems. Prog Coll Pol Sci S. 1998;108:99–104.
56. Borné J, Nylander T, Khan A. Phase behavior and aggregate formation for the aqueous monoolein system mixed with sodium oleate and oleic acid. Langmuir. 2001;17(25):7742–51.
57. Pitzalis P, Monduzzi M, Krog N, Larsson H, Ljusberg-Wahren H, Nylander T. Characterization of the liquid − crystalline phases in the glycerol monooleate/diglycerol monooleate/water system. Langmuir. 2000;16(15):6358–65.
58. Levinger NE, Swafford LA. Ultrafast dynamics in reverse micelles. Annu Rev Phys Chem. 2009;60:385–406.
59. Geil B, Feiweier T, Pospiech EM, Eisenblatter J, Fujara F, Winter R. Relating structure and translational dynamics in aqueous dispersions of monoolein. Chem Phys Lipids. 2000;106(2):115–26.
60. Mahoney MW, Jorgensen WL. Diffusion constant of the TIP5P model of liquid water. J Chem Phys. 2001;114:363–6.
61. Holz M, Heil SR, Sacco A. Temperature-dependent self-diffusion coefficients of water and six selected molecular liquids for calibration in accurate 1H NMR PFG measurements. Phys Chem Chem Phys. 2000;2(20):4740–2.
62. Eriksson PO, Lindblom G. Lipid and water diffusion in bicontinuous cubic phases measured by Nmr. Biophys J. 1993;64(1):129–36.
63. Cuine JF, Charman WN, Pouton CW, Edwards GA, Porter CJ. Increasing the proportional content of surfactant (Cremophor EL) relative to lipid in self-emulsifying lipid-based formulations of danazol reduces oral bioavailability in beagle dogs. Pharm Res. 2007;24(4):748–57.
64. Anby MU, Williams HD, McIntosh M, Benameur H, Edwards GA, Pouton CW, *et al*. Lipid digestion as a trigger for supersaturation: evaluation of the impact of supersaturation stabilization on the in vitro and in vivo performance of self-emulsifying drug delivery systems. Mol Pharm. 2012;9(7):2063–79.
65. Williams HD, Anby MU, Sassene P, Kleberg K, Bakala-N'Goma J-C, Calderone M, et al. Toward the establishment of standardized in vitro tests for lipid-based formulations. 2. The effect of bile salt concentration and drug loading on the performance of type I, II, IIIA, IIIB, and IV formulations during in vitro digestion. Mol Pharm. 2012;9(11):3286–300.
66. Kaukonen A, Boyd B, Charman W, Porter C. Drug solubilization behavior during in vitro digestion of suspension formulations of poorly water-soluble drugs in triglyceride lipids. Pharm Res. 2004;21(2):254–60.